Eur. Phys. J. D (2020) 74: 49
https://doi.org/10.1140/epjd/e2020-100547-2

THE EUROPEAN PHYSICAL JOURNAL D

Regular Article

Velocity imaging of H^- from formic acid: probing functional group dependence in dissociative electron attachment*

N. Bhargava Ram[1,2,a], Vaibhav S. Prabhudesai[1,b], and E. Krishnakumar[1,3,c]

[1] Tata Institute of Fundamental Research, Mumbai 400005, India
[2] Indian Institute for Science Education and Research, Bhopal 462066, India
[3] Raman Research Institute, Bangalore 560080, India

Received 30 October 2019 / Received in final form 11 February 2020
Published online 17 March 2020

Abstract. Dissociative electron attachment (DEA) to formic acid is investigated using velocity slice imaging of H^- ions. From the momentum distributions, we infer that the broad peak observed in absolute cross section of H^- between 6 and 12 eV has contribution from three resonances. The resonance below 7 eV shows angular distribution fairly close to that seen from the B_1 resonance in water and the first peak of the two peaks from the hydroxyl site of acetic acid. The resonance observed around 9 eV appears to have definite contribution from the C-site of the molecule, as identified from the momentum distribution and similarity with other organic molecules including methane. The analysis of the kinetic energy distribution shows that the two resonances below 8 eV are dominated by the contribution from hydroxyl site of the molecule. The results indicate that formic acid tends to behave like other small carboxylic acids and alcohols and displays functional group dependence and corresponding site specificity in the DEA process, to a large extent.

1 Introduction

Electron induced chemistry plays a major role in a large number of cutting edge technologies in semiconductor industry, pollution control, medicine and in planetary atmospheres and astrochemistry [1–3]. The idea of controlling chemical reactions by electrons is being increasingly reinforced by a number of systematic experiments on dissociative electron attachment (DEA) process in molecules [1,2]. One level of control that has been demonstrated is based on the thermodynamic threshold energy corresponding to the production of a specific anion fragment. DEA below this energy necessarily gives selectivity against that particular fragment. Several molecules, in particular poly-atomics show this feature and site specific fragmentation has been demonstrated in them [4–7]. A second, more general level of control using DEA has been discovered, where the control is based on the functional groups present in a molecule [8,9] and does not depend on the threshold energy for different dissociation channels. Here the control arises from the formation of core excited resonances. This involves excitation of an electron at a particular site producing one hole and two particle system, with a propensity for localization of both energy and charge at that site in the molecule. The subsequent fragmentation takes place at the site where the energy and charge are localized [8]. Since each of the functional groups in molecules have characteristic excitation energies as seen in their absorption spectra [10], the resonant attachment and subsequent dissociation take place close to these excitation energies. Thus by changing electron energy, one could selectively break C-H, N-H or O-H bonds in molecules [8,9]. It was also proposed that the dynamics of these fragmentation processes starting from electron attachment is akin to those in the precursor molecules of the respective functional groups [8,9].

A number of other experiments have shown site selective fragmentation through DEA depending on the constituent functional groups. Selective ejection of hydride ion from N-H site, C-H site from methyl group or that from the ring in thymine and uracil were demonstrated with partially deuterated molecules [11,12]. DEA processes characteristic of the O-H and C-O bonds and resulting site and energy selectivity have been observed in a number of alcohols and asymmetric ethers [13–15]. Functional group dependence of DEA for thio group and phenyl sites and N-H site in aromatic amines has also been observed in recent measurements at our lab [16,17]. H^- formation from H_2S and the S-H site in thioacetic acid is found to have very close similarity in terms of resonances and their

* Contribution to the Topical Issue "Low-Energy Positron and Positronium Physics and Electron-Molecule Collisions and Swarms (POSMOL 2019)", edited by Michael Brunger, David Cassidy, Saša Dujko, Dragana Marić, Joan Marler, James Sullivan, Juraj Fedor.

[a] e-mail: nbhargavram@iiserb.ac.in
[b] e-mail: vaibhav@tifr.res.in
[c] e-mail: krishnakumar@rri.res.in

energies [16]. Also, recent studies on benzene, aniline and benzyl amine have shown selective ejection of H^- ions from the C-H and N-H sites arising from functional group dependence in the DEA process [17].

While functional group based site selective fragmentation by DEA has been demonstrated in small carboxylic acids, alcohols and amines [8,9], there are no reports probing this effect in formic acid. More importantly, H^- formation from acetic acid, propanoic acid, methanol and ethanol shows three distinct resonances in the energy range 6−12 eV with the two lowest energy ones arising from the O-H site, like the two main resonances in H_2O. However, in formic acid the H^- channel in this energy range shows a single broad peak with a shoulder at higher energy. The rising edge of this peak shows a structure [18]. The question is, if the functional group dependence does exist, why formic acid behaves in the way it does? Or does the peak observed in the H^- channel have contributions from multiple resonances? While measurements using partial deuteration can identify the O-H and C-H sites, how does one distinguish between two resonances from the same O-H site? These questions are best answered by the use of momentum imaging of fragment ions as we demonstrate here. DEA to Cl_2 is an excellent example where momentum imaging of the fragment anion clearly showed two distinct resonances on either side of a single broad peak in the ion yield curve [19]. The momentum distribution of the ions also provides information as to what extent the functional group dependence is contributing to the dynamics of the DEA process.

Being the simplest carboxylic acid, formic acid is an ideal prototype for understanding DEA in larger molecules of biological interest. It was also found to be the ideal system for testing the catalytic action of free electrons [20]. Mass spectra of negative ions and the ion yield curves for various negative ions other than H^- arising from DEA in formic acid were measured by Pelc et al. [21,22] identifying three resonances at 1.25 eV, 7.5 eV and 9.2 eV respectively. These measurements found the dominant channel to be H-abstraction forming $HCOO^-$ taking place at the 1.2 eV resonance. The two higher energy resonances were found to give OH^- (7.5 eV) and O^- (7.5 eV and 9.2 eV), but with considerably smaller cross sections. Absolute cross sections for all these ions were measured by Prabhudesai et al. [18]. More importantly, it was observed that H^- formation was the dominant process above 5 eV. The low energy resonance has been studied in considerable detail experimentally using selective deuteration [23] and theoretically [24–28]. A summary of these describing the dynamics of this resonance has been given by Fabrikant et al. [2].

2 Experimental setup

The velocity slice imaging experiment used here has been described in detail in an earlier paper [29]. Briefly, the setup consists of a magnetically collimated and pulsed electron beam and an effusive gas beam from a capillary array intersecting perpendicularly. The fragment ions produced are extracted along the direction of the effusive beam towards a position sensitive detector with appropriate electrostatic focusing in a time of flight spectrometer. The electric field needed in the interaction region for extracting and velocity focusing the ions is in pulsed form and is allowed to be present only after the electron pulse so that the electron energy and direction of propagation are not disturbed. The focusing conditions ensure that all ions of same species with same velocity are imaged onto the same point on the detector irrespective of their point of origin in a finite interaction region. The ions are detected using a position sensitive detector made of three 50 mm diameter microchannel plates in Z-stack and a wedge and strip analyser and the associated electronics. The time of arrival and position of each ion is stored in list mode. The velocity slice is obtained by analysing the data off-line by using appropriate time windows, so that a narrow central slice of the Newton sphere is obtained. The imaging of the ions takes place in the presence of a magnetic field of about 40 Gauss. This results in the bending of the ion trajectories when extracted towards the detector and especially is problematic when imaging light and fast moving ions like H^-. However, we could image H^- ions up to 5 eV kinetic energy under these conditions. The electron energy spread in these measurements is about 0.6 eV and this causes a spread in the energy distribution of the H^- ions. The pulsed extraction field was put on 70 ns after the 130 ns wide electron pulse.

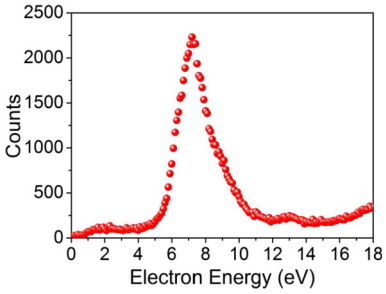

Fig. 1. Ion yield curve of H^- from DEA to formic acid.

The capillary array used for producing the effusive beam was made of 40 micron diameter capillaries with a length of 5 mm. The vapours of the formic acid sample are introduced via these capillaries with a backing pressure of 0.1 mbar as measured in a capacitance manometer. The base pressure in the vacuum chamber in the presence of the effusive beam was $\sim 1 \times 10^{-6}$ mbar. The gas line was kept at 60°C. These conditions ensure that target beam has very little contribution from the formic acid dimer [18,22]. Special care was taken to prevent any water vapour contamination in the formic acid sample (stated purity of 98−100% with acetic acid as the main impurity) by ensuring absolutely leak free gas line. The base vacuum of 3×10^{-8} mbar also prevented any significant contribution from background impurities.

3 Results and discussion

The ion yield curve of H^- from HCOOH given in Figure 1 shows an asymmetric resonance structure peaking at

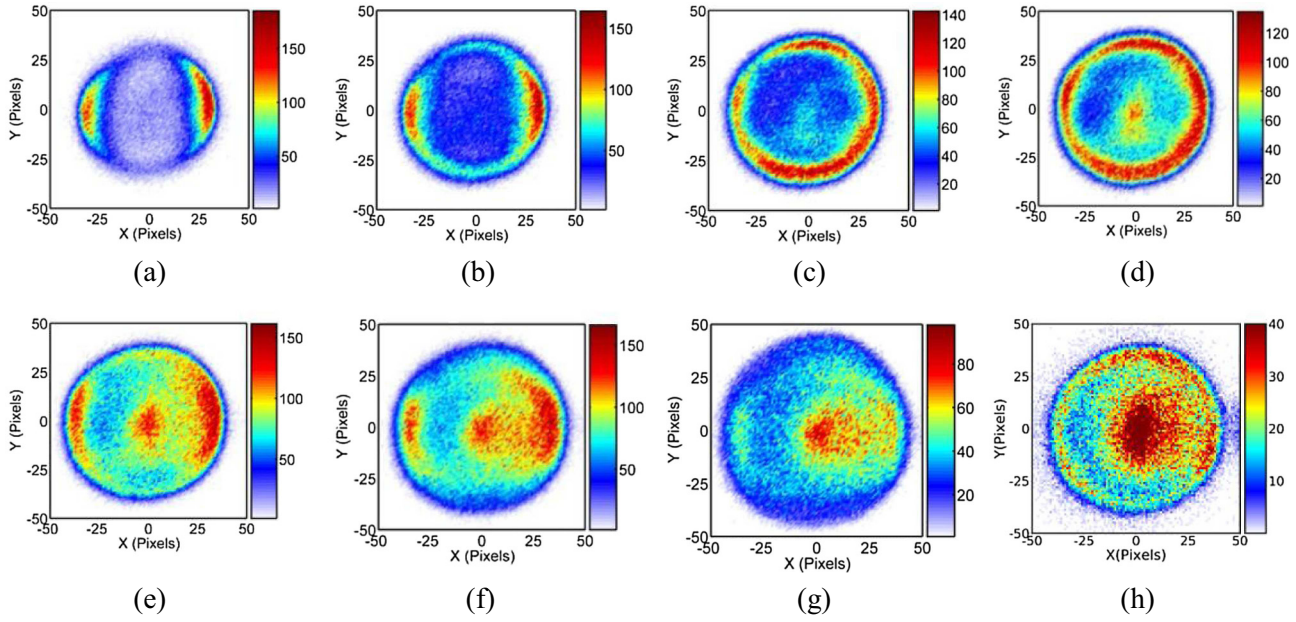

Fig. 2. H^- velocity slice images at different electron energies. The electron beam direction is from top to bottom in all the images. (a) 6.2 eV, (b) 6.7 eV, (c) 7.2 eV, (d) 7.7 eV, (e) 8.3 eV, (f) 8.8 eV, (g) 9.6 eV, and (h) 12.9 eV.

7.3 eV. This is very similar to the relative shape reported earlier for H^- [18], except for slightly inferior electron energy resolution. One may discern the presence of a structure on the rising edge at about 6.5 eV and another clearer one around 9 eV on the falling edge. We also find the small peak at 13 eV that was seen in the previous report [18]. We believe that the small peak centred at 2 eV is due to some impurity since the energy threshold for formation of H^- from formic acid is 3.43 eV [18].

The velocity slice images taken at various incident electron energies in the range 6−10 eV along with one at 12.9 eV are shown in Figure 2. At 6.2 eV we observe a single ring with maximum intensity approximately along right angles to the electron beam and with very little intensity in the forward and backward directions. As the electron energy is increased to 6.7 eV the ring appears to get filled in the forward and backward directions, with maximum intensity still in the 90° direction. At 7.2 eV, which is close to the peak of the resonance structure, the ring is almost isotropic and continues to have this behaviour even at 7.7 eV. As the electron energy reaches 8.3 eV, the isotropy seems to be changing again with more intensity at about right angles. The intensity at 90° becomes more prominent with increase in electron energy till about 8.8 eV and then falls at higher energies. One may also note the development of an inner blob from about 7.2 eV onwards which continues to be present at higher energies and gets pronounced from 8.3 eV onwards. The left-right asymmetry that we see in the images from 8.3 eV onwards is due to the distortion resulting from the effect of the electron beam collimating magnetic field on the H^- ion trajectories. The magnetic field shifts the trajectories of the ions away from the axis of the flight tube making the right half of the Newton sphere coming closer to the edge of the ion optics electrodes, resulting in the distortion. However, the redundancy provided by the cylindrical symmetry about the electron beam allows us to ignore the right half which is affected by the magnetic field and use only the left half in all the analyses.

From the images we can clearly discern three distinct patterns as a function of electron energy: (i) below 7 eV (ii) between 7 and 8 eV and (iii) around 9 eV. This is striking considering the relatively poor electron energy resolution and that tails on either sides of the energy distribution could washout possible distinctions. This indicates that there are three distinct negative ion resonances contributing to the DEA signal, since the angular distribution is dependent on the symmetries of the resonances. The presence of three resonances in formic acid above 6 eV is consistent with other carboxylic acids and small alcohols reported earlier [8,9,13]. We analyse the velocity slice images for the kinetic energies and angular distributions as given below.

The kinetic energy distributions obtained from the velocity map images are shown in Figure 3. The most probable kinetic energy (peak position in the kinetic energy distribution) as a function of electron energy is plotted in Figure 4. As seen in the figure, the most probable kinetic energy increases with electron energy up to 8.3 eV. It increases further after a marginal drop at 8.8 eV. Another aspect of the kinetic energy distribution (Fig. 3) is the rather abrupt increase in the width of the distribution at 8.8 eV and 9.6 eV. This in a way adds to the uncertainty in determining the most probable kinetic energy plotted in Figure 4. In principle, the H^- ions could emanate from the dissociation of either the CH bond or the OH bond in HCOOH. The appearance energy for H^- from the C-site and O-site are 3.43 eV and 3.79 eV respectively [18]. Correspondingly, the maximum kinetic energy of H^- ions produced via these channels at incident elec-

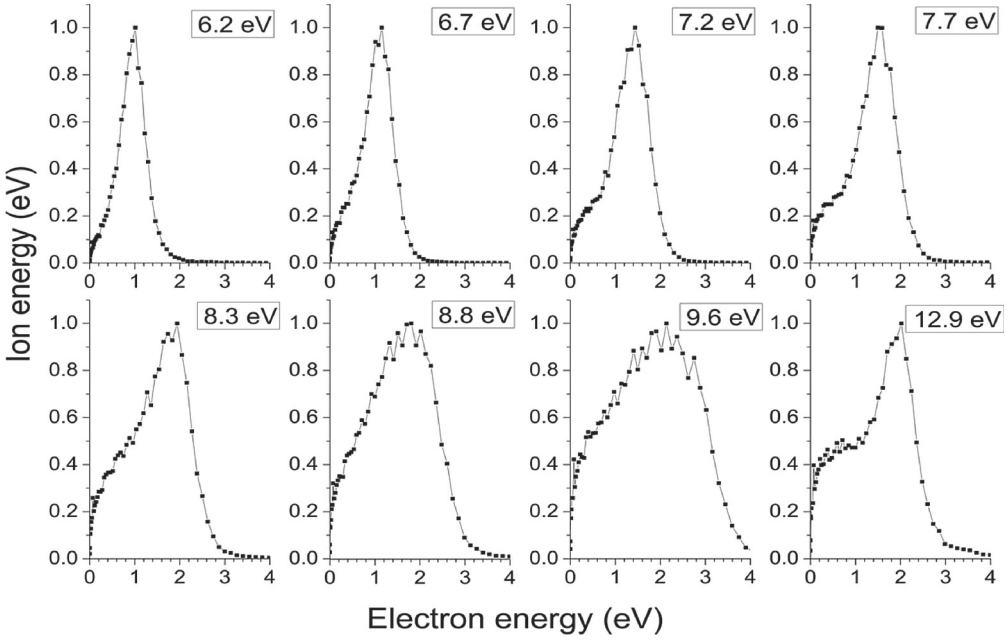

Fig. 3. Kinetic energy distribution of H^- at different electron energies.

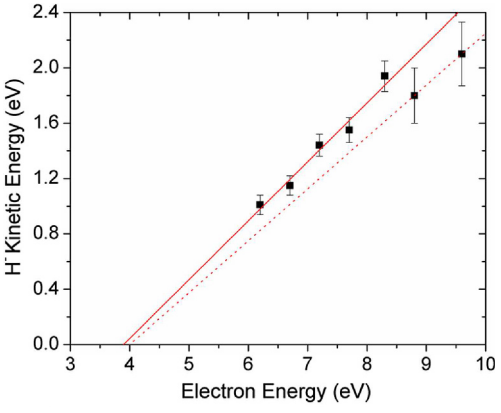

Fig. 4. Most probable kinetic energy of H^- ions as a function of electron energy. Squares are the measured energies and the solid line shows the fit to points up to electron energy of 8.3 eV. The dotted line is the line joining the two high energy points.

tron energy of 6.2 eV will be close to 2.8 eV and 1.7 eV respectively, considering the fact that almost 98% of the available kinetic energy will be in the H^- ions due to the conservation of momentum. At higher electron energies one expects proportional increase in the maximum possible kinetic energy. The peaks in the kinetic energy distribution are well below the maximum allowed kinetic energies. The position and width of the peaks in the kinetic energy distribution show that the neutral fragment is formed with internal excitation.

Figure 4 shows that there are two distinct slopes in the most probable kinetic energy vs electron energy plots. We believe that the break in the kinetic energy plot giving two different slopes as well as distinct difference in the kinetic energy distribution is a clear indication of the difference in the dynamics leading to H^- formation. The best fit straight line for the points up to 8.3 eV electron energy meets the electron energy axis at 3.9 eV, which is in excellent agreement with the threshold for H^- formation from the O-H site. The line joining the last points, which has a different slope meets the x-axis at 4 eV. This also is not too far from the threshold for the H^- formation from the O-H site. Here, we find that even a small/marginal 0.1 eV shift in either of the data points can substantially change the x-intercept. Besides, this fit is based on just two points. The threshold for formation of H^- from the C-site is 3.4 eV. A clear distinction for this warrants measurements using partially deuterated samples.

The central blob seen in the images beyond 7.7 eV corresponds to near zero kinetic energy. This implies that all the excess energy is being used up in the internal excitation of the neutral fragment or three-body fragmentation. Considering the amount of internal excitation needed to give such low energy blob, it is quite likely that the dissociation dynamics involves a few-body fragmentation, giving rise to H^- and two neutral fragments. The three-body dissociation channels for formic acid involving the formation of H^- are $H + CO_2 + H^-$, $OH + CO + H^-$ and $O + CHO + H^-$. The respective threshold energies are 3.65 eV, 4.7 eV and 8.46 eV. Four-body fragmentations occur above 9 eV. One would expect considerable kinetic energy release in the first two channels, if the excess energy is not partitioned into internal excitation of the neutral molecular fragments. The near-zero energy central blobs we see in the images are possible, only if almost all the excess energy goes into internal excitation. The fact that the blob appears strongly only above 8 eV favours the third channel with the threshold of 8.46 eV as its source. The presence of the blob below this energy may be explained as due to finite energy spread of the electron beam and its high energy tail.

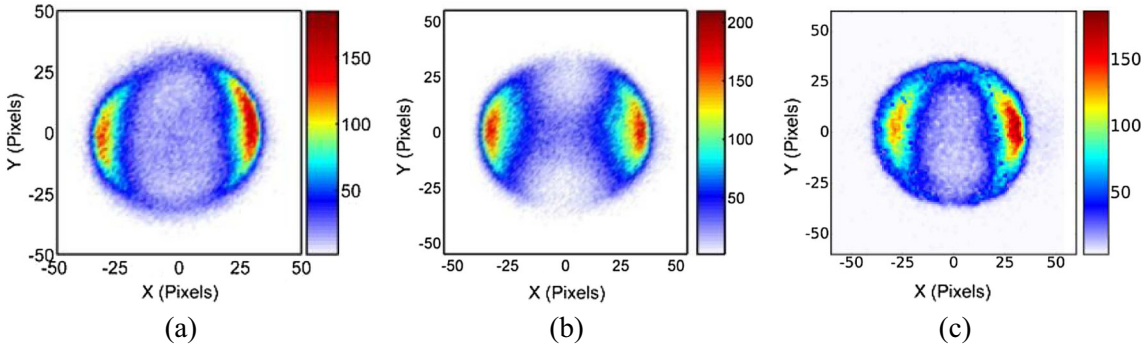

Fig. 5. Velocity slice images of H^- from HCOOH at 6.2 eV (a), H^- from H_2O at 6.5 eV (adapted from Ref. [31]) (b) and H^- from CH_3COOH at 6.7 eV (c). The electron beam direction is from top to bottom in all three.

DEA measurements on partially deuterated acetic acid has shown that the highest energy resonance observed in the H^- channel arises predominantly from the C-H site and two lower energy ones from the O-H site [8]. This has been substantiated further by the studies on alcohols and ethers in which it was shown that the resonance arising from the excitation at the C-site is responsible for the production of negative ions at the highest energy among the three Feshbach resonances in all these molecules [13–15]. Moreover, the site selectivity observed in pyrimidine bases shows clear distinction between the resonances arising from excitation at the C-site, O-site and N-site, including that between the C-site in the aromatic ring or the methyl part [11,12]. Based on these, one may argue that the resonance seen in formic acid around 9 eV is a Feshbach resonance formed by excitation of an electron at the C-site. One important aspect of DEA arising from localization at the C-site is the few-body fragmentation that is always present, as seen in the case of methane, to begin with [30]. Apart from a two-body fragmentation channel producing H^- as manifested by a ring of appreciable kinetic energy in the momentum distribution, the DEA in methane gives very low energy H^- which has been shown to be due to three-body fragmentation [30]. A comparison of the velocity slice images around 9 eV (Figs. 2e, 2f, and 2g) shows similarity with that observed in methane, including the central blob arising from three-body fragmentation. This behaviour of three-body fragmentation at the C-site has been observed in the production of anions that necessarily need multi-bond scission in several systems and seems to be a characteristic of the DEA centred at the C-site [9,13,17]. Thus one may conclude that the central blob seen around 9 eV is arising from the C-H site, while the contribution from the O-H site to the outer ring cannot be ruled out. We also do not know if any sort of scrambling of H atom is present between the two sites.

Based on the velocity slice images (Fig. 2), we concluded above that there are three resonances contributing to the H^- ion yield curve. The images from the rising edge of the peak show dominant intensity distribution peaking around 90°. This is markedly seen at 6.2 eV. The one at 6.7 eV seems to have an isotropic contribution, similar to that seen at 7.2 eV. This isotropic contribution could be due to the finite electron energy resolution causing a mixing of the signals from 7.2 eV and/or due to overlapping nature of the resonances. The image at 6.2 eV has a close resemblance with that of H^- from H_2O at 6.5 eV, as shown in Figure 5. Also given in the figure is the velocity slice image of H^- from CH_3COOH taken at 6.7 eV. It has been shown that H^- from acetic acid at this energy is exclusively formed from the hydroxyl site in acetic acid [8,9]. The resonance at 6.5 eV is the dominant one in water and is known to have B_1 symmetry. The angular distribution of the H^- from water peaks at 100° [31]. The calculation of the entrance channel amplitude is also consistent with this [32]. Both experiment and theory show that the electron approaching H_2O at an angle almost perpendicular to the plane of the molecule. The B_1 resonance arises from the excitation of the lone pair electron of O and is responsible for the functional group dependence and site specificity seen in the DEA at the hydroxyl sites in various molecules. This effect is undoubtedly seen in acetic acid [8] and is seen in the angular distribution data as well. The angular distributions corresponding to the images in Figure 5 are given in Figure 6. The angular distribution peaks at about 90° for formic acid and 100° for acetic acid in comparison to 100° for water. Both formic acid and acetic acid have increasing intensities towards the two poles, though overall distribution in formic acid seems to be closer to that of water. The ejection of H^- at almost 90° shows that the electron is approaching at an angle perpendicular to the O-H bond. The similarity in the angular distribution between acetic acid and formic acid and with that of water shows that the resonance at the rising edge of the H^- ion yield curve in formic acid is centred at the O-site and not the C-site. This is consistent with the conclusions based on kinetic energy analysis discussed above.

The kinetic energy distribution of H^- from formic acid at 6.2 eV and 6.7 eV is shown in Figure 7 along with the kinetic energy distribution for H^- from water at 6.5 eV. The kinetic energy distributions from formic acid peak between 1 and 1.2 eV (threshold 3.79 eV) whereas that from water peak at 1.7 eV (threshold 4.42 eV). Lower kinetic energy observed in the case of formic acid may be due to the availability of more degrees of freedom in the neutral fragment. The distinctly different kinetic energy distributions also rules out any possible role of water as an impurity in the formic acid sample contributing to the H^- signal at these energies.

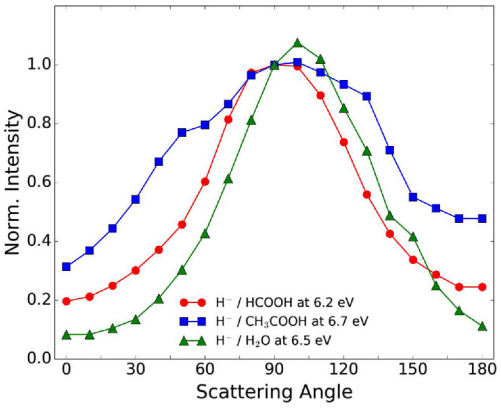

Fig. 6. Angular distribution of H^- ions from HCOOH at 6.2 eV (circles), CH_3COOH at 6.7 eV (squares) and H_2O at 6.5 eV (triangles) corresponding to the images shown in Figure 5.

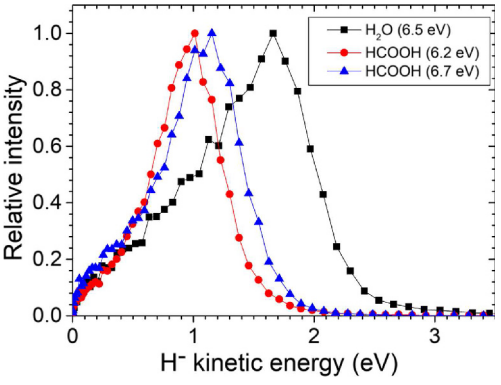

Fig. 7. Comparison of kinetic energy distribution of H^- from water at 6.5 eV (squares) (adapted from Ref. [31]) to that from formic acid at 6.2 eV (circles) and 6.7 eV (triangles).

The analysis of the images around the peak in the ion yield curve (7.2 to 8.3 eV) in order to probe the site specificity is rather difficult due to two main reasons. First one is the difficulty in separating contributions from resonances on either side of it. The finite electron energy resolution of the experiment adds further difficulty to it. The second one is the difficulty in comparing the entrance channel amplitude for formic acid at this resonance with that of the A_1 resonance in water at 8.5 eV. For A_1 resonance in water, the entrance channel amplitude peaks in the plane of the molecule along the principal axis [33]. Moreover, it has been found that the axial recoil approximation for this resonance in water does not hold good [33–35] due to dominant bending mode vibrations. Considering all this, exact calculations of the entrance channel amplitude in formic acid would be needed to make any reasonable attempt in looking for functional group dependence based on angular distribution around the peak of the ion yield curve. However, the plot of most probable kinetic energy as a function of electron energy shown in Figure 4 clearly shows that the H^- formed at this resonance is being ejected from O-site.

The peak at 13 eV in the ion yield curve was observed in earlier experiments [18]. The energy range falls into the polar dissociation region leading to the $H^- + COOH^+$ channel (threshold: 11.63 eV). The blob in the centre of Figure 2h is attributed to this channel. The outer ring in Figure 2h, which is isotropic in character, gives the most probable kinetic energy as 2 eV. This may be due to a resonance process, which may be undergoing multiple bond dissociation. That the H^- has relatively low energy of 2 eV indicates the formation of an H atom along with other neutrals with possible electronic excitation.

4 Summary

We have obtained velocity slice images of H^- ions formed from formic acid in the 6 to 13 eV range. The images across the broad peak in the 6 eV to 10 eV range in the ion yield curve show the presence three distinct resonances, which could be correlated with structures seen in the curve. Presence of three distinct resonances in this energy interval is similar to what has been observed in other carboxylic acids and small alcohols. An analysis of the kinetic energy peak position as a function of electron energy shows that the two lower energy resonances correspond to formation of H^- from the O-site. The angular distribution of H^- at 6.2 eV shows strong resemblance to that from the 6.5 eV resonance in H_2O and H^- from the first of the three Feshbach resonances seen in acetic acid. This allows us to conclude that the resonance is centred at the O-H site in the molecule and corresponds to lone pair excitation at the O-atom. At the third resonance around 9 eV we see near-zero energy ions from a three-body dissociation process, which is a characteristic of the C-site, though we are unable to rule out contribution from the O-site at this energy. Based on these results, we conclude that the functional group dependence and the consequent site specific fragmentation observed in DEA is active in formic acid as well to a fair degree. A weak resonance observed at 13 eV, which is lying in the dipolar dissociation continuum appears to decay through multiple bond dissociation, giving several neutrals including an H atom.

EK acknowledges Raja Ramanna fellowship from Department of Atomic Energy, India. VSP acknowledges Department of Atomic Energy, India for financial support.

Author contribution statement

EK and VSP conceived the idea, NBR did the measurements and all the authors contributed to the analysis and preparation of the manuscript.

References

1. O. Ingólfsson, *Low Energy Electrons – Fundamentals and Applications* (Pan Stanford, Singapore, 2019)
2. I.I. Fabrikant, S. Eden, N.J. Mason, J. Fedor, Adv. Atom. Mol. Opt. Phys. **66**, 545 (2017)

3. L.G. Christophorou, D.L. McCorkle, A.A. Christodoulides, in *Electron-molecule Interactions and their Applications*, edited by L.G. Christophrous (Academic Press, New York, 1984), Chap. 6, Vol. 1
4. H. Abdul–Carime, S. Gohlke, E. Illenberger, Phys. Rev. Lett. **92**, 168103 (2004)
5. I. Bald, J. Kopyra, E. Illenberger, Angew. Chem. Int. Ed. **45**, 4851 (2006)
6. S. Ptasińska, S. Denifl, P. Scheier, E. Illenberger, T.D. Märk, Angew. Chem. Int. Ed. **44**, 6941 (2005)
7. S. Denifl, P. Sulzer, A. Mauracher, M. Probst, T.D. Märk, P. Scheier, Phys. Scr. **78**, 058101 (2008)
8. V.S. Prabhudesai, D. Nandi, A.H. Kelkar, E. Krishnakumar, Phys. Rev. Lett. **95**, 143202 (2005)
9. V.S. Prabhudesai, D. Nandi, A.H. Kelkar, E. Krishnakumar, J. Chem. Phys. **128**, 154309 (2008)
10. M.B. Robin, in *Higher Excited States of Polyatomic Molecules* (Academic Press, New York, 1975), Vol. 2
11. S. Ptasińska, S. Denifl, V. Grill, T.D. Märk, E. Illenberger, P. Scheier, Phys. Rev. Lett. **95**, 093201 (2005)
12. S. Ptasińska, S. Denifl, B. Mroz, M. Probst, V. Grill, E. Illenberger, P. Scheier, T.D. Märk, J. Chem. Phys. **123**, 124302 (2005)
13. B.C. Ibănescu, O. May, A. Monney, M. Allan, Phys. Chem. Chem. Phys. **9**, 3163 (2007)
14. B.C. Ibănescu, M. Allan, Phys. Chem. Chem. Phys. **11** 7640 (2009)
15. B.C. Ibănescu, M. Allan, Phys. Chem. Chem. Phys. **10**, 5232 (2008)
16. K. Gope, E. Krishnakumar, V.S. Prabhudesai (2020), in preparation
17. V.S. Tadsare, E. Krishnakumar, V.S. Prabhudesai (2020), in preparation
18. V.S. Prabhudesai, D. Nandi, A.H. Kelkar, R. Parajuli, E. Krishnakumar, Chem. Phys. Lett. **405**, 172 (2005)
19. K. Gope, V.S. Prabhudesai, N.J. Mason, E. Krishnakumar, J. Phys. B: At. Mol. Opt. Phys. **49**, 015201 (2016)
20. D. Davis, S. Kundu, V.S. Prabhudesai, Y. Sajeev, E. Krishnakumar, J. Chem. Phys. **149**, 064308 (2018)
21. A. Pelc, W. Sailer, P. Scheier, M. Probst, N.J. Mason, E. Illenberger, T.D. Märk, Chem. Phys. Lett. **361**, 277 (2002)
22. A. Pelc, W. Sailer, P. Scheier, N.J. Mason, E. Illenberger, T.D. Märk, Vacuum **70**, 429 (2003)
23. R. Janeckova, D. Kubala, O. May, J. Fedor, M. Allan, Phys. Rev. Lett. **111**, 213201 (2013)
24. F.A. Gianturco, R.R. Luchesse, New J. Phys. **6**, 66 (2004)
25. T.N. Rescigno, C.S. Trevisan, A.E. Orel, Phys. Rev. Lett. **96**, 21320 (2006)
26. T.N. Rescigno, C.S. Trevisan, A.E. Orel, Phys. Rev. A **80**, 046701 (2009)
27. G.A. Gallup, P.D. Burrow, I.I. Fabrikant, Phys. Rev. A **79**, 042701 (2009)
28. G.A. Gallup, P.D. Burrow, I.I. Fabrikant, Phys. Rev. A **80**, 046702 (2009)
29. D. Nandi, V.S. Prabhudesai, E. Krishnakumar, A. Chatterjee, Rev. Sci. Instrum. **76**, 053107 (2005)
30. N.B. Ram, E. Krishnakumar, Chem. Phys. Lett. **511**, 22 (2011)
31. N.B. Ram, V.S. Prabhudesai, E. Krishnakumar, J. Phys. B: At. Mol. Opt. Phys. **42**, 225203 (2009)
32. D.J. Haxton, C.W. McCurdy, T.N. Rescigno, Phys. Rev. A **73**, 062724 (2006)
33. H. Adaniya, B. Rudek, T. Osipov, D.J. Haxton, T. Weber, T.N. Rescigno, C.W. McCurdy, A. Belkacem, Phys. Rev. Lett. **103**, 233201 (2009)
34. N.B. Ram, V.S. Prabhudesai, E. Krishnakumar, Phys. Rev. Lett. **106**, 049301 (2011)
35. N.B. Ram, V.S. Prabhudesai, E. Krishnakumar, J. Chem. Sci. **124**, 271 (2012)